

Conformational Heterogeneity of Arylamine-Modified DNA: ¹⁹F NMR Evidence

Li Zhou,[†] Masoumeh Rajabzadeh,[‡] Daniel D. Trafficante,[‡] and Bongsup P. Cho*[†]

Contribution from the Departments of Biomedical Sciences and Chemistry, University of Rhode Island, Kingston, Rhode Island 02881

Received September 17, 1996. Revised Manuscript Received April 17, 1997[®]

Abstract: One- and two-dimensional ¹⁹F NMR spectroscopy was used to investigate the conformational heterogeneity of two arylamine-modified DNA duplexes, d[CTTCTTG*ACCTC]·d[GAGGTCAAGAAG], in which G* is either *N*-(deoxyguanosin-8-yl)-4'-fluoro-4-aminobiphenyl (dG-C8-FABP) (**I**) or *N*-(deoxyguanosin-8-yl)-7-fluoro-2-aminofluorene (dG-C8-FAF) (**II**). The ¹⁹F NMR spectrum of **I** showed a single peak, while that of **II** revealed two prominent signals with a 55:45 ratio, in good agreement with previous ¹H NMR results (Cho *et al. Biochemistry* **1992**, *31*, 9587–9602; **1994**, *33*, 1373–1384). Slow interconversion between the two conformations of **II** was established by temperature-dependent two-dimensional ¹⁹F NMR chemical exchange spectra. On the basis of magnetic anisotropy effects and isotopic solvent-induced shifts, the ¹⁹F signals at –117.31 and –118.09 ppm in the ¹⁹F NMR spectrum of **II** were assigned to a relatively undisturbed “B-type” conformer and a highly perturbed “stacked” conformer, respectively. Analysis of the temperature dependent (5–40 °C) line shapes by computer simulation yielded an interconversion barrier (ΔG^\ddagger) of 14.0 kcal/mol with a chemical exchange time of 2 ms at 30 °C. This new ¹⁹F approach should be very useful in investigating the sequence-dependent conformational heterogeneity of arylamine-modified DNA.

Introduction

Arylamines and amides are an important class of chemical carcinogens, some of which induce tumors in experimental animals and in humans.¹ Among the most extensively studied arylamines are 4-aminobiphenyl (ABP) and 2-aminofluorene (AF)^{1–3} and their analogs. DNA is considered to be a principal target for the activated derivatives of these carcinogens, which

form covalent adducts *in vivo* to give rise to C8-substituted deoxyguanosine adducts as the major and the most persistent forms (dG-C8-ABP and dG-C8-AF, respectively, Figure 1).¹ Elucidation of three-dimensional molecular structures of DNA containing these adducts is crucial to understanding the differences in their mutagenic and carcinogenic outcomes.^{4–6,7m}

* To whom correspondence should be addressed. Phone: (401) 874-5024. Fax: (401) 874-2181. E-mail: bcho@uriacc.uri.edu.

[†] Department of Biomedical Sciences.

[‡] Department of Chemistry.

[®] Abstract published in *Advance ACS Abstracts*, June 1, 1997.

(1) Beland, F. A.; Kadlubar, F. F. In *Handbook of Experimental Pharmacology*; Cooper, C. S., Grover, P. L., Eds.; Vol 94/I, Springer-Verlag: Heidelberg, 1990; pp 267–325.

(2) Kriek, E. J. *Cancer Res. Clin. Oncol.* **1992**, *118*, 481–489.

(3) Heflich, R. H.; Neft, R. E. *Mutat. Res.* **1994**, *318*, 73–174.

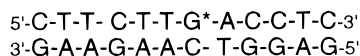
(4) Harris, T. M.; Stone, M. P.; Harris, C. M. *Chem. Res. Toxicol.* **1988**, *1*, 79–96.

(5) (a) Patel, D. J. *Curr. Opin. Struct. Biol.* **1992**, *2*, 345–353. (b) Krugh, T. R. *Curr. Opin. Struct. Biol.* **1994**, *4*, 351–364.

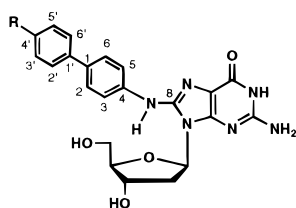
(6) Geacintov, N. E.; Cosman, M.; Hingerty, B. E.; Amin, S.; Broyde, S.; Patel, D. J. *Chem. Res. Toxicol.* **1997**, *10*, 111–146.

(7) (a) Norman, D.; Abuaf, P.; Hingerty, B. E.; Live, D.; Grunberger, D.; Broyde, S.; Patel, D. J. *Biochemistry* **1989**, *28*, 7462–7476. (b) Cho, B. P.; Beland, F. A.; Marques, M. M. *Biochemistry* **1992**, *31*, 9587–9602. (c) O'Handley, S. F.; Sanford, D. G.; Xu, R.; Lester, C. C.; Hingerty, B. E.; Broyde, S.; Krugh, T. R. *Biochemistry* **1993**, *32*, 2481–2497. (d) Cho, B. P.; Beland, F. A.; Marques, M. M. *Biochemistry* **1994**, *33*, 1373–1384. (e) Eckel, L. M.; Krugh, T. R. *Nat. Struct. Biol.* **1994**, *1*, 89–94. *Biochemistry* **1994**, *33*, 13611–13624. (f) Shapiro, R.; Sidawi, D.; Miao, Y.-S.; Hingerty, B. E.; Schmidt, K. E.; Moskowitz, J.; Broyde, S. *Chem. Res. Toxicol.* **1994**, *7*, 239–253. (g) Abuaf, P.; Hingerty, B. E.; Broyde, S.; Grunberger, D. *Chem. Res. Toxicol.* **1995**, *8*, 369–378. (h) Shapiro, R.; Ellis, S.; Hingerty, B. E.; Broyde, S. *Chem. Res. Toxicol.* **1995**, *8*, 117–127. (i) Milhe, C.; Dhalluin, C.; Fuchs, R. P. P.; Lefèvre, J.-F. *Nucleic Acids Res.* **1994**, *22*, 4646–4652. (j) Milhe, C.; Fuchs, R. P. P.; Lefèvre, J.-F. *Eur. J. Biochem.* **1996**, *235*, 120–127. (k) Mao, B.; Cosman, M.; Hingerty, B. E.; Broyde, S.; Patel, D. J. *Biochemistry* **1995**, *34*, 6226–6238. (l) Mao, B.; Hingerty, B. E.; Broyde, S.; Patel, D. J. *Biochemistry* **1995**, *34*, 16641–16653. (m) Broyde, S.; Hingerty, B. E. *Biopolymers* **1983**, *22*, 2423–2441.

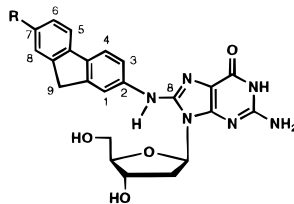
(8) (a) Mao, B.; Vyas, R. R.; Hingerty, B. E.; Broyde, S.; Basu, A. K.; Patel, D. J. *Biochemistry* **1996**, *35*, 12659–12670. (b) Cosman, M.; de los Santos, C.; Fiala, R.; Hingerty, B. E.; Singh, S. B.; Ibanez, V.; Margulis, L. A.; Live, D.; Geacintov, N. E.; Broyde, S.; Patel, D. J. *Proc. Natl. Acad. Sci. U.S.A.* **1992**, *89*, 1914–1918. (c) de los Santos, C.; Cosman, M.; Hingerty, B. E.; Ibanez, V.; Margulis, L. A.; Geacintov, N. E.; Broyde, S.; Patel, D. J. *Biochemistry* **1992**, *31*, 5245–5252. (d) Cosman, M.; de los Santos, C.; Fiala, R.; Hingerty, B. E.; Ibanez, V.; Luna, E.; Harvey, R. G.; Geacintov, N. E.; Broyde, S.; Patel, D. J. *Biochemistry* **1993**, *32*, 4145–4155. (e) Cosman, M.; Hingerty, B. E.; Luneva, N.; Amin, S.; Geacintov, N. E.; Broyde, S.; Patel, D. J. *Biochemistry* **1996**, *35*, 9850–9863. (f) Fountain, M. A.; Krugh, T. R. *Biochemistry* **1995**, *34*, 3152–3161. (g) Cosman, M.; Xu, R.; Hingerty, B. E.; Amin, S.; Harvey, R. G.; Geacintov, N. E.; Broyde, S.; Patel, D. J. *Biochemistry* **1995**, *34*, 6247–6260. (h) Cosman, M.; Fiala, R.; Hingerty, B. E.; Amin, S.; Geacintov, N. E.; Broyde, S.; Patel, D. J. *Biochemistry* **1994**, *33*, 11507–11517. (i) Cosman, M.; Fiala, R.; Hingerty, B. E.; Amin, S.; Geacintov, N. E.; Broyde, S.; Patel, D. J. *Biochemistry* **1994**, *33*, 11518–11527. (j) Cosman, M.; Fiala, R.; Hingerty, B. E.; Laryea, A.; Lee, H. Harvey, R. G.; Amin, S.; Geacintov, N. E.; Broyde, S.; Patel, D. J. *Biochemistry* **1993**, *32*, 12488–12497. (k) Cosman, M.; Laryea, A.; Fiala, R.; Hingerty, B. E.; Amin, S.; Geacintov, N. E.; Broyde, S.; Patel, D. J. *Biochemistry* **1995**, *34*, 1295–1307. (l) Cosman, M.; Hingerty, B. E.; Geacintov, N. E.; Broyde, S.; Patel, D. J. *Biochemistry* **1995**, *34*, 15334–15350. (m) Schurter, E. J.; Sayer, J. M.; Oh-hara, T.; Yeh, H. J. C.; Yagi, H.; Luxon, B. A.; Jerina, D. M.; Gorenstein, D. G. *Biochemistry* **1995**, *34*, 9009–9020. (n) Schurter, E. J.; Yeh, H. J. C.; Sayer, J. M.; Lakshman, M. K.; Yagi, H.; Jerina, D. M.; Gorenstein, D. G. *Biochemistry* **1995**, *34*, 1364–1375. (o) Yeh, H. J. C.; Sayer, J. M.; Liu, X.; Altieri, A. S.; Ryrd, R. A.; Lakshman, M. K.; Yagi, H.; Schurter, E. J.; Gorenstein, D. G.; Jerina, D. M. *Biochemistry* **1995**, *34*, 13570–13581. (p) Feng, B.; Voehler, M.; Zhou, L.; Passarelli, M.; Harris, C. M.; Harris, T. M.; Stone, M. P. *Biochemistry* **1996**, *35*, 7316–7329. (q) Belguise-Valladier, P.; Fuchs, R. P. P. *Biochemistry* **1991**, *30*, 10091–10100. (r) Koehl, P.; Valladier, P.; Lefèvre, J.-F.; Fuchs, R. P. P. *Nucleic Acids Res.* **1989**, *17*, 9531–9541. (s) Veaute, X.; Fuchs, R. P. P. *Nucleic Acids Res.* **1991**, *19*, 5603–5606. (t) Seeberg, E.; Fuchs, R. P. P. *Proc. Natl. Acad. Sci. U.S.A.* **1990**, *87*, 191–194. (u) Rodriguez, H.; Loechler, E. L. *Biochemistry* **1993**, *32*, 1759–1769. (v) Drouin, E. E.; Lech, J.; Loechler, E. L. *Biochemistry* **1995**, *34*, 2251–2259. (w) Jelinsky, S.; Liu, T.; Geacintov, N. E.; Loechler, E. L. *Biochemistry* **1995**, *34*, 13545–13553.



- (I) $G^* = \text{dG-C8-FABP}$
 (II) $G^* = \text{dG-C8-FAF}$



- R = H: **dG-C8-ABP**
 R = F: **dG-C8-FABP**



- R = H: **dG-C8-AF**
 R = F: **dG-C8-FAF**

Figure 1. Chemical structures of the C8-substituted deoxyguanosine adducts and the base sequence of the modified 12-mer in which the carcinogen is covalently attached at the C8-position of G^* (I, FABP-modified 12-mer duplex, $G^* = \text{dG-C8-FABP}$; II, FAF-modified 12-mer duplex, $G^* = \text{dG-C8-FAF}$). Key: dG-C8-ABP, *N*-(deoxyguanosin-8-yl)-4-aminobiphenyl; dG-C8-FABP, *N*-(deoxyguanosin-8-yl)-4'-fluoro-4-aminobiphenyl; dG-C8-AF, *N*-(deoxyguanosin-8-yl)-2-aminofluorene; dG-C8-FAF, *N*-(deoxyguanosin-8-yl)-7-fluoro-2-aminofluorene.

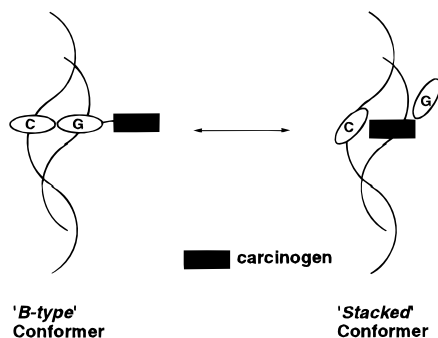


Figure 2. Schematic representations of the B-type conformer and the stacked conformer observed for an aminofluorene-modified DNA duplex.

We^{7b,d} and others^{7e} have shown that arylamine-modified DNA duplexes adopt two major prototype conformations: namely, a "B-type" conformer, in which the carcinogen resides in the major groove of a relatively undistorted B-DNA, and a "stacked" conformer, in which the carcinogen is inserted into the helix at the adduct site (Figure 2). Due to the highly perturbed nature of the DNA adduct at the modification site, the stacked conformer is considered as a promutagenic conformer.^{7d,e} These experimental findings are in accord with previous theoretical predictions, which have suggested several possible AF-induced dynamic states in DNA.^{7m} Such conformational heterogeneity appears to be commonly associated with a wide range of carcinogen-modified DNA adducts⁶⁻⁸ and is strongly modulated by the nature (coplanarity, stereochemistry, *etc.*) of the carcinogens,^{8a-p} as well as the base sequence context surrounding the adduct.^{7a,d,f-1,8a,e,f,l,p-w} For example, the population of the promutagenic stacked conformer increases as the planarity of the carcinogen increases: ABP (~10%)^{7b} < AF (~50%)^{7d,e}

< AP (1-aminopyrene, ~100%).^{8a} This is presumably due to differences in the stacking abilities of the carcinogen fragments,⁹ which may account for the lower frameshift mutagenicity of dG-C8-ABP in *Salmonella typhimurium* TA 1538 and for the relative resistance of the same adduct as compared to dG-C8-AF to DNA repair enzymes in the livers of dogs.¹⁰ Recent mutation studies by Melchior *et al.*¹¹ using plasmid pBR322 transfected into *Escherichia coli* have shown that the highly planar AP produces an unusually high incidence of frameshifts, and also a much higher mutational efficiency per adduct as compared to the less planar ABP, further substantiating the stacking argument.

Conformational heterogeneity appears to be the basis for the diverse nature of adduct-initiated mutagenesis.^{6,7,8a,e,f,k,l,n,o-w} Since mutagenesis is a relatively infrequent biological event and DNA adducts adopt multiple conformations, it is conceivable that observed mutations are due to the replication of an adduct in a minor conformation.¹² Until now, ¹H NMR spectroscopy has been used as a principal tool to investigate the solution structure of carcinogen adducts in DNA.⁴⁻⁸ However, when an adduct induces multiple conformations, as is often the case for carcinogen-modified DNA, ¹H NMR data are extremely difficult to interpret owing to spectral complexities and chemical exchanges. It is therefore not surprising that prior NMR structural studies of carcinogen-modified DNA have focused mostly on the major conformations.^{6,7a-f,i-1,8a,d-f,k-p} This necessitates the development of novel techniques, in which one can correlate mutations to a specific adduct conformation.¹²

In this paper, we have explored ¹⁹F NMR spectroscopy as an alternate method that takes advantage of the sensitivity of the ¹⁹F chemical shifts to the tertiary structural environment of nucleic acids.¹³⁻¹⁶ The approach has been to prepare two DNA duplexes containing fluorine-tagged model carcinogens (I and II, Figure 1), and to investigate their static and dynamic ¹⁹F NMR characteristics.

Results and Discussion

Design of the Fluorine Probes. The model fluorine probes chosen for the present study were two 12-mer DNA duplexes containing either *N*-(deoxyguanosin-8-yl)-4'-fluoro-4-aminobiphenyl (dG-C8-FABP) or *N*-(deoxyguanosin-8-yl)-7-fluoro-2-aminofluorene (dG-C8-FAF) (I and II, respectively, Figure 1). Incorporation of fluorine at the longest axis (*i.e.*, 4'-position of ABP and 7-position of AF) has been shown to maintain carcinogenicity in rat livers, while the activity toward other tissues is comparable to that of the parent compound.^{1,17,18} The DNA adduct profiles of FABP, FAF, and their corresponding nonfluoro compounds are also similar.¹⁹ According to circular

(9) Shapiro, R.; Underwood, G. R.; Zawadzka, H.; Broyde, S.; Hingerty, B. E. *Biochemistry* **1986**, *25*, 2198-2205.

(10) Beland, F. A.; Beranek, D. T.; Dooley, K. L.; Heflich, R. H.; Kadlubar, F. F. *Environ. Health Prospect.* **1983**, *49*, 125-134.

(11) Melchior, W. B. Jr.; Marques, M. M.; Beland, F. A. *Carcinogenesis* **1994**, *15*, 889-899.

(12) Loechler, E. L. *Carcinogenesis* **1996**, *17*, 895-902.

(13) Craik, D. J. *NMR in Drug Design*; CRC Press: Boca Raton, FL, 1996.

(14) Gerig, J. T. *Methods Enzymol.* **1989**, *177*, 3-23.

(15) Lu, P.; Metzler, W. J.; Rastinejad, F.; Wasilewski, J. In *Structure and Function of Nucleic Acids and Proteins*; Wu, F. Y.-H., Wu, C.-W., Eds.; Raven Press: New York, 1990; pp 19-35.

(16) Rastinejad, F.; Evilla, C.; Lu, P. *Methods Enzymol.* **1995**, *261*, 560-574.

(17) Arcos, J. C.; Argus, M. F. *Chemical Induction of Cancer*; Academic Press: New York, 1974; Vol. IIB.

(18) Miller, J. A.; Sandin, R. B.; Miller, E. C.; Rusch, H. P. *Cancer Res.* **1956**, *15*, 188-199.

(19) Fuchs, R. P. P.; Lefèvre, J.-F.; Pouyet, J.; Daune, M. P. *Biochemistry* **1976**, *15*, 3347-3351.

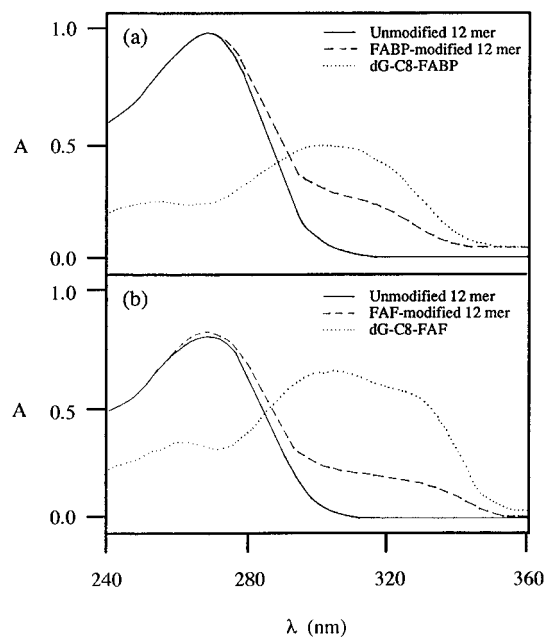


Figure 3. Ultraviolet spectra of (a) dG-C8-FABP and the unmodified and FABP-modified 12-mer and (b) dG-C8-FAF and the unmodified and FAF-modified 12-mer, in the 240–360 nm range, monitored using a photodiode array detector.

dichroism^{19,20} and molecular modeling²¹ studies, dG-C8-FAF and dG-C8-AF exert similar conformational alterations in DNA. The 12-mer sequence (d[CTTCTTGACCTC]·d[GAGGTCAA-GAAG], Figure 1) employed in this study is essentially that of the original 15-mer (d[TACTCTTCTTGACCT]·d[AGGTCAA-GAAGAGTA]) used in our previous ¹H NMR work,^{7b,d} but shortened to facilitate synthetic and spectral work without perturbing the unique conformational features at the adduct site.

Preparation of the Fluorine Probes. The synthesis, purification, and chemical characterization of the monomeric dG adducts (dG-C8-FABP and dG-C8-FAF, Figure 1) were carried out by application of the general method of Lee and King.²² The synthesis involves a treatment of dG with the reactive *N*-acetoxy-*N*-(trifluoroacetyl) derivatives of 4'-fluoro-4-aminobiphenyl and of 7-fluoro-2-aminofluorene, with concomitant solvolysis of the trifluoroacetyl fragment to produce the deacetylated arylamine adduct at the C8 position of guanine. The UV characteristics of the monomeric dG-C8-FABP and dG-C8-FAF adducts (Figure 3) are similar to those of the corresponding nonfluoro analogs.^{23,24} The ¹H NMR spectra of these monomeric adducts have been analyzed by COSY experiments and by comparison with the ¹H NMR spectra of the corresponding nonfluoro parent adducts.^{25,26} The ¹H NMR spectrum of dG-C8-FABP exhibited all the resonances of dG (except for the H8) and four groups of aromatic signals integrating for eight protons, which is in good agreement with that reported by van de Poll *et al.* for the same adduct.²⁵ Likewise, the ¹H NMR spectral pattern of dG-C8-FAF was very similar to that of dG-C8-AF reported by Beland *et al.*,²⁶ except for the lack of a high-field H7 aromatic signal. The ¹⁹F NMR spectra of the dG-C8-

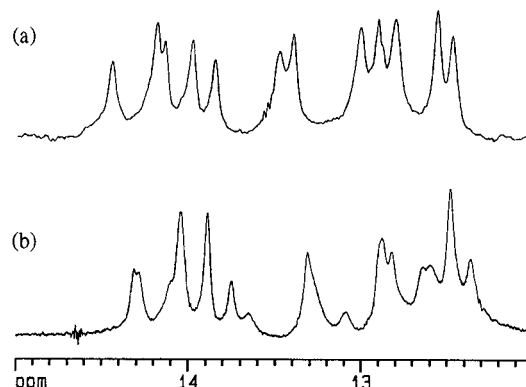


Figure 4. ¹H NMR (400 MHz, 1D) spectra (12–15 ppm) of (a) the FABP- (I) and (b) the FAF-modified (II) 12-mer duplexes in 90% H₂O/10% D₂O at 18 °C. The spectra were recorded using a 1–1 jump and return pulse sequence²⁸ and referenced relative to DSS (2,2-dimethyl-2-silapentane-5-sulfonate, sodium salt).

FABP and dG-C8-FAF adducts exhibited characteristic multiplets at −119.56 and −120.03 ppm, respectively.

The FABP- and FAF-modified 12-mers (d[CTTCTTG*ACCTC], G* = dG-C8-FABP and dG-C8-FAF, respectively) were similarly prepared as described for the nonfluoro ABP- and AF-modified 15-mer DNA oligomers.²⁴ The UV spectra (Figure 3) of the modified 12-mers exhibited a broad shoulder above 300 nm, which is characteristic of the extended conjugation expected from DNA containing C8-substituted arylamine adducts.²⁴ HPLC analysis of an enzymatic hydrolysate of the FABP-12-mer to nucleosides displayed several peaks, one of which was distinctively nonpolar and identified as dG-C8-FABP on the basis of comparison of its UV spectrum and retention time with those of a standard (*vide supra*). The FAF-modified 12-mer was characterized in a similar manner.

Optical Melting Curves. Optical melting curves of the unmodified, FABP- and FAF-modified (I and II, Figure 1) duplexes at 5 μM concentration showed a typical cooperative helix–coil transition upon heating. The midpoint transition temperatures (*T*_m) were found to be 46 ± 1, 36 ± 1, and 35 ± 1 °C for the unmodified, FABP-modified (I), and FAF-modified (II) duplexes, respectively. As compared to the 15-mer sequences containing nonfluoro analogs,²⁴ the *T*_m values were slightly higher for the unmodified 12-mer, and relatively unchanged for the modified duplexes, while the extent of the adduct-induced thermal destabilization (10–11 °C) was similar. The addition of a G:C pair at both the 5'- and 3'-terminals of the 12-mer sequence may account for their relative stability.

Thermodynamic parameters for the three duplexes were calculated at 25 °C using the procedure of Markey and Breslauer:²⁷ unmodified 12-mer, Δ*H*[°] = −5.2 kcal/mol, Δ*S*[°] = 22.8 eu, Δ*G*[°] = −12.0 kcal/mol; FABP-duplex (I), Δ*H*[°] = −5.2 kcal/mol, Δ*S*[°] = 18.4 eu, Δ*G*[°] = −10.7 kcal/mol; FAF-duplex (II), Δ*H*[°] = −4.1 kcal/mol, Δ*S*[°] = 20.9 eu, Δ*G*[°] = −10.3 kcal/mol. The values calculated for II may not be accurate since it involves a conformational exchange in the duplex state (*vide infra*). Despite the significant thermal destabilization, the small difference in free energy (ΔΔ*G*[°] < 1.7 kcal/mol) between the unmodified and modified 12-mer duplexes suggests that the adduct-induced helix destabilization is relatively minimal.

NMR Studies. Figure 4 shows the imino proton spectra of the FABP- and FAF-modified 12-mer DNA duplexes (I and II, respectively) taken in H₂O buffer at 18 °C. While I showed the 12 expected sharp imino protons in the downfield region

(20) Lefèvre, J.-F.; Fuchs, R. P. P.; Daune, M. P. *Biochemistry* **1978**, *17*, 2561–2567.

(21) Broyde, S.; Hingerty, B. *Chem.-Biol. Interact.* **1983**, *47*, 69–78.

(22) Lee, M.-S.; King, C. M. *Chem.-Biol. Interact.* **1981**, *34*, 239–244.

(23) Shibutani, S.; Gentles, R.; Johnson, F.; Grollman, A. P. *Carcinogenesis* **1991**, *12*, 813–818.

(24) Marques, M. M.; Beland, F. A. *Chem. Res. Toxicol.* **1990**, *3*, 559–565.

(25) van de Poll, M. L. M.; Tijdens, R. B.; Vondráček, P.; Bruins, A. P.; Meijer, D. K. F.; Meerman, J. H. N. *Carcinogenesis* **1989**, *10*, 2285–2291.

(26) Beland, F. A.; Allaben, W. T.; Evans, F. E. *Cancer Res.* **1980**, *40*, 834–840 (1980).

(27) Markey, L. A.; Breslauer, K. J. *Biopolymers* **1987**, *26*, 1601–1620.

(28) Sklenor, V.; Bax, A. *J. Magn. Reson.* **1987**, *74*, 469–479.

(29) Bodenhausen, G.; Kogler, H.; Ernst, R. R. *J. Magn. Reson.* **1984**, *58*, 370–388.

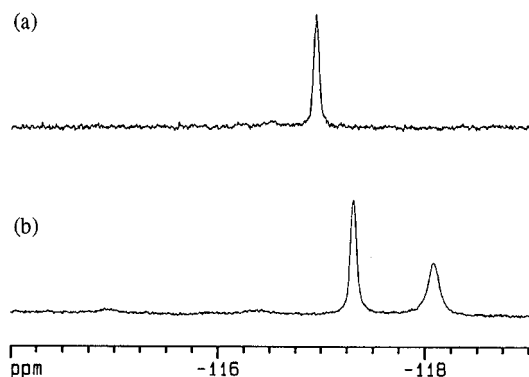


Figure 5. ^{19}F NMR spectra (376.5 MHz) of (a) **I** and (b) **II** taken in 90% $\text{H}_2\text{O}/10\%$ D_2O at 18 °C, referenced to external CFCl_3 .

(Figure 4a), the same sequence containing dG-C8-FAF (**II**) exhibited at least 15 resolvable imino proton resonances with varying degrees of intensity (Figure 4b). These results indicate that **I** exists primarily in a single conformation and **II** adopts multiple conformations. In line with this interpretation, the ^{19}F NMR spectrum of **I** revealed a single resonance at -116.94 ppm (Figure 5a), while that of **II** exhibited two prominent signals at -117.31 and -118.09 ppm (Figure 5b), each representing a unique fluorine environment. Their intensity ratio was 55:45, in good agreement with previous ^1H NMR results^{7d} that showed the presence of an approximately equal distribution of the B-type and stacked conformers in a similar sequence context.

The conformational relationship between the two ^{19}F signals in the spectrum of **II** was established by temperature-dependent NOESY/EXSY experiments. Figure 6a shows contour plots of two-dimensional ^{19}F NMR exchange spectra of **II** recorded at 18 °C, where the off diagonal cross peaks indicate a transfer of magnetization from one conformer to another. When an identical measurement was conducted at 5 °C (Figure 6b), no such cross peaks were detected. This strong temperature dependence³⁰ confirms that the two signals arise *via* chemical exchange from two structurally distinct, slowly-interconvertible conformations, presumably a B-type conformer and a stacked conformer.

On the basis of magnetic anisotropy effects and isotopic solvent-induced shifts, the upfield signal (-118.09 ppm) in the spectrum of **II** was assigned to that arising from the stacked conformer. The large shift ($+0.78$ ppm, Figure 5b) relative to that assigned to the B-type conformer (-117.31 ppm) can be attributed to ring-current effects produced by intercalation of the carcinogen moiety into the helix as depicted in Figure 2. A comparable magnitude of shielding through this mechanism has been observed for 5-fluorouracil residues located in helical regions of tRNA.³¹ Such an intercalation also limits the motion of the carcinogenic moiety, thus resulting in signal broadening. More direct and compelling evidence for this assignment was obtained by observing a H–D isotope effect.³² As a result of the interaction of the exposed fluorine with the solvent, the ^{19}F resonance from the accessible FAF residue of the B-type conformer was shifted upfield by 0.24 ppm when the deuterium content of the solvent was increased from 10% to 100%. In contrast, the chemical shift of the buried (intercalated) fluorine resonance in the stacked conformer was relatively unchanged ($+0.08$ ppm) upon the same solvent change. As expected, the -116.94 ppm signal in the spectrum of **I** (Figure 5a), which adopts predominantly a B-type conformation, exhibited a similar shielding ($+0.23$ ppm) under the same conditions.

(30) Wemmer, D. E. In *Biological Magnetic Resonance*; Berliner, L. J., Reuben, J. Eds.; Plenum Press: New York, 1992; Vol. 10, pp 195–264.

(31) Hardin, C. C.; Gollnick, P.; Kallenbach, N. R.; Cohn, M.; Horowitz, J. *Biochemistry* **1986**, 25, 5699–5709.

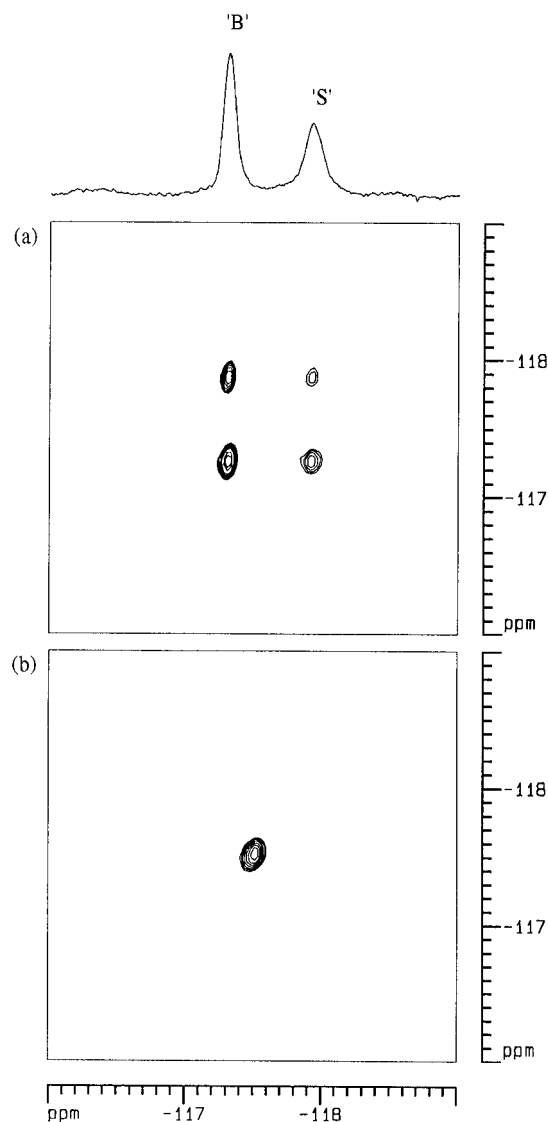


Figure 6. ^{19}F NMR (2D) exchange spectra of **II** recorded in 100% D_2O at (a) 18 °C and (b) 5 °C. The spectra were obtained in the phase-sensitive mode using a NOESY sequence:²⁹ sweep width 4529 Hz, number of complex data points in t_2 512, number of complex free induction decays in t_1 128, number of scans 480, number of dummy scans 16, recycle delays 1.0 s, and mixing time 400 ms. The data were subjected to exponential apodization using a line broadening of 8 Hz in both dimensions and then zero-filled before Fourier transformation of the 512×256 data matrix. The data were not symmetrized. A slight chemical shift difference of the downfield signal was due to a temperature effect (see Figure 7): **B** = B-type conformer; **S** = stacked conformer.

The spin–lattice relaxation times (T_1 values) in H_2O buffer were also measured to gain further insight into the relaxation nature of the two conformers of **II**. We anticipated that the exposed fluorine of the B-type conformer would have a shorter T_1 as compared to that of the buried fluorine of the stacked conformer, due to a relatively large dipolar contribution to the relaxation from the solvent protons.³³ Unexpectedly, the -117.31 ppm ^{19}F signal of the B-type conformer had a T_1 of 0.48 s, while that (-118.09 ppm) belonging to the stacked conformer had a T_1 of 0.52 s. The lack of significant difference in the T_1 values between the two conformers suggests that intercalation of the carcinogen into the helix occurs without complete exclusion of solvent molecules, or that the fluorine nucleus is relaxed by mechanisms other than dipolar relaxation.

(32) Hansen, P. E.; Dettman, H. D.; Sykes, B. D. *J. Magn. Reson.* **1985**, 62, 487–496.

(33) O'Connor, T. P.; Coleman, J. E. *Biochemistry* **1982**, 21, 848–854.

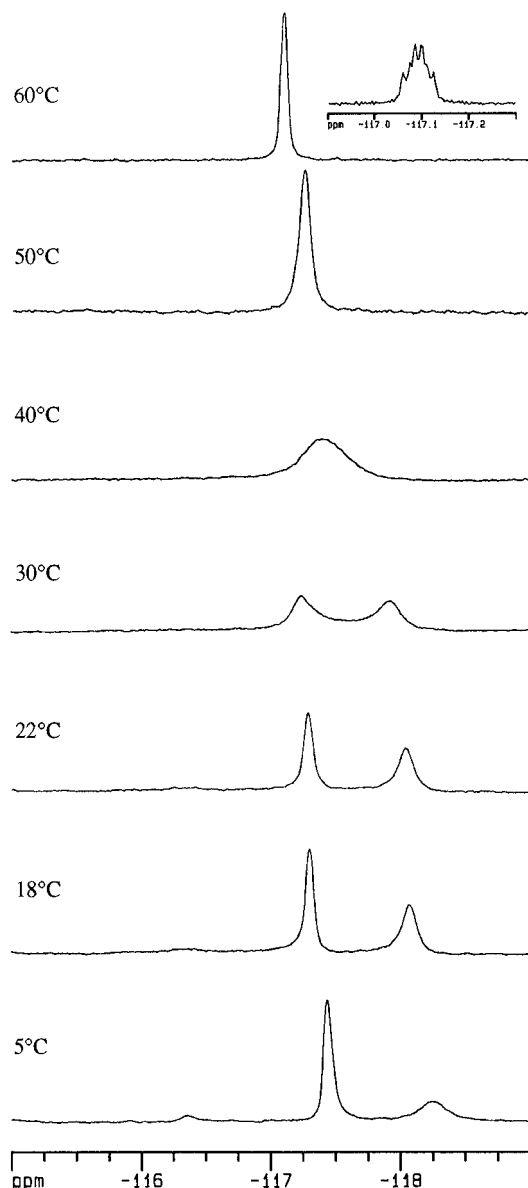


Figure 7. Temperature-dependent ^{19}F NMR spectra of **II** in 90% $\text{H}_2\text{O}/10\%$ D_2O . The temperature range was 5–60 °C. Before Fourier transformation, all data were apodized with an exponential window function using a line-broadening factor of 5 Hz, except for the inset spectrum at 60 °C, for which a Lorentzian to Gaussian resolution enhancement (LB = -1 Hz and GB = 0.2) was used. The inset shows fine H–F splitting patterns of a rapidly rotating FAF moiety.

The dynamic interconversion between the B-type conformer and the stacked conformer of **II** was probed by temperature-dependent ^{19}F NMR spectroscopy.^{34,35} The results of 376.5 MHz ^{19}F NMR are shown in Figure 7. While the two fluorine signals were in slow exchange at 5 °C, they became exchange broadened and moved closer together as the temperature was raised, giving rise to one time-averaged coalescent signal (-117.43 ppm) at 40 °C. The two signals showed line-shape changes characteristic of a two-site exchange process, in which the population of the stacked conformer increased steadily with increasing temperature. Analysis of the temperature-dependent (5–40 °C) line shapes by computer simulation yielded the activation parameters for exchange: $\Delta G^\ddagger(30\text{ °C}) = 14.0$ kcal/mol, $\Delta H^\ddagger = 16.0$ kcal/mol, and $\Delta S^\ddagger = 6.7$ eu. The rates of interconversion of the two conformers at 18 and 30 °C were

(34) Friebohn, H. *Basic One- and Two Dimensional NMR Spectroscopy*, 2nd ed.; VCH Publishers: New York, 1993; pp 263–291.

(35) Sandström, J. *Dynamic NMR Spectroscopy*; Academic Press: London, 1982.

found to be 76 and 500 s^{-1} , which are equivalent to chemical exchange lifetimes of 13 and 2 ms, respectively. On further raising of the temperature, the coalescent peak became sharper, and eventually narrowed at 60 °C (-117.10 ppm), showing fine H–F splitting patterns (inset in Figure 7), which indicates a rapidly rotating FAF moiety in a single-strand 12-mer.

The dynamic energetic results obtained for the FAF-modified 12-mer duplex (**II**) suggest that the conformeric equilibrium between the B-type and the stacked conformers is physiologically accessible; thereby, repair enzymes are likely to be confronted with the two conformations *in vivo*. This situation has been previously labeled as a “two-way” mutagenic switch by Eckel and Krugh.^{7c} In a similar manner, the term “three-way” mutagenic switch was used to describe mutations derived from a duplex containing propanodeoxyguanosine (PdG) opposite a -2 deletion site in the *hisD3052* sequence, in which the possibilities include successful bypass of PdG, miscoding leading to base substitution, or strand slippage leading to a frameshift mutation.³⁶

Conclusions

In this report we present conclusive evidence that the FABP-12 mer (**I**) exists exclusively as a B-type conformer, while the FAF-12 mer (**II**) adopts a 55:45 mixture of the B-type and stacked conformers at room temperature. While detailed structural interpretation of ^{19}F NMR is limited, the sensitivity of ^{19}F chemical shifts to the DNA helix environment clearly offers unique advantages, especially in dealing with multiple conformations that are commonly associated with carcinogen-modified DNA. With this ^{19}F approach, one should be able to monitor the conformeric ratio as a function of the base sequence surrounding the adduct site, the pH, and the salt concentrations, all of which are important factors in predicting mutagenic outcomes. Such data will hopefully provide valuable quantitative insights about the role of conformational heterogeneity in arylamine carcinogenesis. This newly developed ^{19}F approach may provide a tool for understanding the conformational basis of site-specific mutagenesis of arylamines and other related carcinogens.

Experimental Section

Warning. *FABP and FAF derivatives are mutagens as well as carcinogens in experimental animals, and should be handled with caution.*

12-mer oligodeoxynucleotides [d(CTTCTTGACCTC)] and [d(GAG-GTCAAGAAG)] were obtained from Keystone Laboratory, Inc. (Menlo Park, CA). HPLC grade solvents were obtained from Fisher Scientific (Pittsburgh, PA). DNase I, phosphodiesterase I, and alkaline phosphatase were purchased from Sigma Chemical Co. (St. Louis, MO). 4-Fluorobiphenyl was purchased from Pfaltz & Bauer, Inc. (Waterburg, CT). All other reagent chemicals were obtained from Aldrich Chemical Co. (Milwaukee, WI).

Melting points were measured using a Büchi melting point apparatus and are uncorrected. Low- and high-resolution electron impact mass spectra (LRMS and HRMS) were obtained on a Finnigan-MAT CH5 and a 731 instrument, respectively, at the University of Illinois Mass Spectrometry Laboratory, Urbana-Champaign, IL. Electrospray mass spectra of monomer dG adducts were measured on a Micromass VG Quattro triple quadrupole mass spectrometer at the Northeastern University Barnett Mass Spectrometry Laboratory, Boston, MA.

HPLC Methods. Samples were concentrated using a Model AES 1000-120 SpeedVac concentrator (Forma Scientific, Inc., Marietta, OH). HPLC data were obtained on a Waters Associates system equipped with Model 501 pumps, a U6K injector, a 680 automated gradient controller, and a Hitachi L-3000 photodiode array detector. Separations were conducted using either an Ultrasphere C18 ODS analytical column

(36) Weisenseel, J. P.; Moe, J. G.; Reddy, G. R.; Marnett, L. J.; Stone, M. P. *Biochemistry* **1995**, *34*, 50–64.

(4.6 × 250 mm, 5 μm) or a semiprep column (10.0 × 250 mm, 5 μm) from Beckman Instruments, Inc., San Ramon, CA, with one of the following systems: system 1, 90% methanol/10% H₂O, isocratic (1 mL/min); system 2, a 60-min linear gradient of 5–35% acetonitrile/0.1 M ammonium acetate (pH 7.0) (2 mL/min); system 3, a 20-min linear gradient of 25–60% acetonitrile/0.1 M ammonium acetate (pH 7.0) (2 mL/min).

NMR Methods. ¹H NMR spectra were obtained on either a DPX400 or AM300 Bruker NMR spectrometer, operating at 400 and 300 MHz, respectively, with tetramethylsilane (TMS) as the internal standard. Chemical shifts for oligomer samples are reported in parts per million downfield from internal 2,2-dimethyl-2-silapentane-5-sulfonate, sodium salt (DSS). ¹⁹F NMR spectra were measured on a DPX400 or AM300 Bruker NMR spectrometer, operating at 376.5 and 282.4 MHz, respectively, and referenced relative to the external CFCl₃. The available 5 mm probes did not allow proton decoupling. ¹⁹F spin-lattice relaxation times (*T*₁) were determined on a Bruker AM300 instrument by using the inversion-recovery method. Two-dimensional exchange experiments were carried out in the phase-sensitive mode using a NOESY pulse sequence.²⁹ Detailed NMR parameters are included in the figure captions.

For NMR experiments, the FABP-modified 12-mer (d[CTTCTTG-(FABP)ACCTC]) was dissolved in a pH 7.0 H₂O buffer containing 100 mM NaCl, 10 mM sodium phosphate, and 100 μM tetrasodium EDTA, and annealed with an equimolar amount of the complementary strand (d[GAGGTCAAGAAG]) to form a 0.6 mM solution of **I**. A 2.5 mM solution of **II** was prepared in a similar manner.

Line Shape Analysis. Theoretical line shapes for a two-site exchange system with different populations were generated by using a Windows program (WinDNMR: Dynamic NMR Spectra for Windows, Version 1.30, J. Chem. Educ. Software Series D, Volume 3, Number 2; Reich, H. J., Department of Chemistry, University of Wisconsin, Madison, WI) and fitted with experimental spectra.^{34,35}

Optical Melting Experiments. Temperature-dependent absorption changes for duplex samples (5 μM) at 260 nm were analyzed on a Hitachi U-2000 spectrophotometer equipped with a Model 9000 Isotemp refrigerated circulator (Fisher Scientific). The midpoint transition temperature (*T*_m) was obtained by the procedure of Markey and Breslauer from the plot of α versus *T*. The *T*_m values are the temperature for α equals 0.5 where α is the fraction of strand in the double helix. At each temperature point, α was calculated from the temperature-dependent UV absorption curve. Thermodynamic parameters (Δ*H*^o, Δ*S*^o, and Δ*G*^o) were calculated using the following equations:²⁷ log *K*_{eq} = -Δ*H*^o/2.3*RT* + Δ*S*^o/2.3*R* and Δ*G*^o = Δ*H*^o - *T*Δ*S*^o, where *K*_{eq} = 2α/*c*(1 - α)²; *c* = 5 × 10⁻⁶ M; *R* = gas constant.

Synthesis of Reactive Carcinogens. *N*-Acetoxy-*N*-(trifluoroacetyl)-4'-fluoro-4-aminobiphenyl was prepared starting from 4'-fluoro-4-nitrobiphenyl by the method of Lee and King:²² HPLC (system 1) *t*_R 3.49 min; ¹H NMR (400 MHz, CDCl₃) δ 8.4–7.2 (m, 8H), 2.27 (s, 3H, -OCH₃); UV λ_{max} 268 nm; LRMS *m/z* 341 (M⁺, 16), 299 (M⁺ - CH₂CO, 27), 282 ([M⁺ - CH₃CO₂], 16), 213 ([M⁺ - CH₃CO₂ - CF₃], 24), 185 (ArN⁺, 45), 171 (Ar⁺, 27), 43 (CH₃CO⁺, 100); HRMS calcd for C₁₆H₁₁NO₃F₄ 341.0675, found 341.0672. The nitro precursor 4'-fluoro-4-nitrobiphenyl was synthesized by nitration of 4-fluorobiphenyl: 1.72 g (10 mmol) of 4-fluorobiphenyl in 100 mL of CH₂Cl₂ was treated with excess N₂O₄ (20 mmol) in CH₂Cl₂ at room temperature. After 24 h, 10 mmol of N₂O₄ was added and the mixture was stirred for an additional 24 h. The excess N₂O₄ was evaporated, and the residue was dissolved in ethyl ether, washed with H₂O, and recrystallized in 95% ethanol to give long white needles: 1.94 g (89%); mp 124.5–125.5 °C (lit.³⁷ mp 120–121 °C); ¹H NMR (300 MHz, CDCl₃) δ 8.31 (d, 2H, H_{3,5}, *J*_{2,3} = 8.9 Hz), 7.70 (d, 2H, H_{2,6}), 7.61 (dd, 2H, H_{2',6'}, *J*_{2',3'} = 8.8 Hz, *J*_{2',F} = 5.1 Hz), 7.20 (dd, 2H, H_{3',5'}, *J*_{3',F} = 9.7 Hz); UV λ_{max} 310 nm. *N*-Acetoxy-*N*-(trifluoroacetyl)-7-fluoro-2-aminofluorene was synthesized in a similar manner from 2-fluoro-7-nitrofluorene (Aldrich Co.): HPLC (system 1) *t*_R 3.69 min; ¹H NMR (400 MHz, CDCl₃) δ 7.8–7.1 (m, 6H), 3.95 (s, 2H, H_{9',9''}), 2.25 (s, 3H, -OCH₃); UV λ_{max} 275 nm; LRMS *m/z* 353 (M⁺, 36), 311 (M⁺ - CH₂CO, 32), 294 ([M⁺ - CH₃CO₂], 39), 225 ([M⁺ - CH₃CO₂ - CF₃], 100), 197 (ArN⁺, 66), 183 (Ar⁺, 56), 43 (CH₃CO⁺, 87); HRMS calcd for C₁₇H₁₁NO₃F₄ 353.0675, found 353.0675.

Synthesis of dG-C8-FABP and dG-C8-FAF. The monomer dG adducts were prepared by following a general literature method,²³ except that the adduct was extracted with ethyl acetate. To a pH 7.0 citrate buffer (10 mM) solution containing dG (10 mg) was added an ethanol solution of the appropriate diester (~25 mg) obtained above. The mixture was stirred at 45 °C under a N₂ atmosphere. After 18 h, the reaction mixture was concentrated to dryness, redissolved in H₂O, and extracted with ethyl ether (3 × 5 mL). The adduct in the aqueous layer was then extracted with ethyl acetate (3 × 5 mL) and isolated by reversed-phase HPLC. The yield was in the range of 10–30%. Data for dG-C8-FABP: HPLC (system 3) *t*_R 16.80 min; UV λ_{max} 305 nm; ¹H NMR (400 MHz, methanol-*d*₄) δ 7.72 (d, 2H, H_{3,5}, *J*_{2,3} = *J*_{5,6} = 8.7 Hz), 7.59 (dd, 2H, H_{2',6'}, *J*_{2',3'} = *J*_{5',6'} = 8.7 Hz, *J*_{2',F} = *J*_{6',F} = 5.6 Hz), 7.50 (d, 2H, H_{2,6}), 7.14 (dd, 2H, H_{3',5'}, *J*_{3',F} = *J*_{5',F} = 8.7 Hz, *J*_{3',5'} = 1.9 Hz), 6.47 (dd, 1H, G_{1'}, *J*_{1',2'} = 9.3 Hz, *J*_{1',2''} = 6.0 Hz), 4.59 (dd, 1H, G_{3'}, *J*_{2',3'} = 6.6 Hz, *J*_{3',4'} = 1.5 Hz), 4.03 (d, 1H, G_{4'}, *J*_{4',5'} = 2.3 Hz), 3.92 (m, 2H, G_{5',5''}), 2.71 (m, 1H, G_{2'}, *J*_{1',2'} = 9.3 Hz, *J*_{2',2''} = -13.4 Hz, *J*_{2',3'} = 6.6 Hz), 2.17 (m, 1H, G_{2''}, *J*_{2',3'} = 1.7 Hz); ¹⁹F NMR (methanol-*d*₄) δ -119.56 ppm (multiplet). Data for dG-C8-FAF: HPLC (system 3) *t*_R 16.93 min; UV λ_{max} 300–335 nm; ¹H NMR (400 MHz, methanol-*d*₄) δ 7.96 (s, 1H, H₁), 7.67 (dd, 1H, H₅, *J*_{5,6} = 8.3 Hz, *J*_{5,F} = 5.0 Hz), 7.64 (d, 1H, H₄, *J*_{3,4} = 8.3 Hz), 7.55 (d, 1H, H₃), 7.25 (d, 1H, H₈, *J*_{8,F} = 9.1 Hz), 7.05 (dd, 1H, H₆, *J*_{5,6} = 8.3 Hz, *J*_{6,F} = 9.3 Hz, *J*_{6,8} = 2.3 Hz), 6.47 (dd, 1H, G_{1'}, *J*_{1',2'} = 9.1 Hz, *J*_{1',2''} = 6.0 Hz), 4.59 (dd, 1H, G_{3'}, *J*_{2',3'} = 6.4 Hz, *J*_{3',4'} = 1.6 Hz), 4.03 (d, 1H, G_{4'}), 3.93 (m, 2H, G_{5',5''}), 3.87 (s, 2H, H₉), 2.72 (m, 1H, G_{2'}, *J*_{1',2'} = 9.1 Hz, *J*_{2',2''} = -13.4 Hz, *J*_{2',3'} = 6.4 Hz), 2.17 (m, 1H, G_{2''}, *J*_{2',3'} = 1.7 Hz); ¹⁹F NMR (methanol-*d*₄) δ -120.03 ppm (multiplet).

The identities of dG-C8-FABP and dG-C8-FAF were also confirmed by electrospray mass spectrometry. The spectrum of dG-C8-FABP showed [M + H]⁺ at *m/z* 453.3 and a fragment ion at *m/z* 337.1, which is consistent with loss of the deoxyribose moiety. Likewise, the spectrum of dG-C8-FAF exhibited peaks at *m/z* 465.6 and 349.4, which correspond to [M + H]⁺ and [MH₂ - dR]⁺, respectively.

Synthesis and Characterization of the FABP-Modified and FAF-Modified 12-mers. The synthesis of the FABP- and FAF-modified 12-mer strand was carried out as described for the corresponding nonfluoro ABP- and AF-modified 15-mers.²⁴ This involved treating d[CTTCTTGACCTC] with the *N*-trifluoroacetyl derivatives of FABP and FAF prepared above. Each modified 12-mer was separated from the unreacted 12-mer by reversed-phase HPLC using system 2. Average yields with greater than 98% sample purity were approximately 10% and 30% for the FABP and FAF-modified 12-mers, respectively (see Figure 3 for their UV spectra). Data for unmodified 12-mer: HPLC *t*_R 17.85 min; UV λ_{max} 268 nm. Data for FABP-modified 12-mer: HPLC *t*_R 24.68 min; UV λ_{max} 268, 295–345 nm (shoulder). Data for FAF-modified 12-mer: HPLC *t*_R 24.36 min; UV λ_{max} 268, 295–350 nm (shoulder). The modified oligonucleotides were further characterized by a standard enzymatic degradation analysis.²⁴ The presence of the nonpolar monomeric dG-C8-FABP or dG-C8-FAF adduct in the enzymatic hydrolysate mixture was confirmed by comparison of their HPLC retention times and UV spectra with those of authentic standards.

Acknowledgment. Dedicated to Professor Elie Abushanab on the occasion of his 60th birthday. We thank Drs. F. A. Beland and M. M. Marques for helpful comments and Dr. Paul Vouros for providing electrospray mass spectra of the monomer adducts. This work was supported by a grant from the American Cancer Society (CN-130).

Supporting Information Available: ¹H NMR spectra of the monomer adducts (dG-C8-FABP and dG-C8-FAF), optical melting profiles of the three 12-mer duplexes (unmodified, **I** and **II**), ¹⁹F NMR spectra of **II** in 10% and 90% D₂O, and a plot of ¹⁹F NMR chemical shifts of **II** as a function of temperature (2 pages). See any current masthead page for ordering and Internet access instructions.